

Tube-based geometries for organic photovoltaics

Yuan Li,¹ Eric D. Peterson,¹ Huihui Huang,^{1,2} Mingjun Wang,^{1,2} Dan Xue,³ Wanyi Nie,¹ Wei Zhou,¹ and David L. Carroll^{1,a)}

¹Department of Physics, Center for Nanotechnology and Molecular Materials, Wake Forest University, Winston-Salem, North Carolina 27109, USA

²Department of Electronic Science and Technology, School of Physical Science and Technology, Wuhan University, Wuhan 430072, People's Republic of China

³Department of Mathematics, Beijing Jiaotong University, Beijing 100044, People's Republic of China

(Received 7 November 2009; accepted 17 May 2010; published online 17 June 2010)

We demonstrate a waveguiding tube-based optical geometry that provides a general approach to improving organic photovoltaic performance. By fabricating bulk-heterojunction photovoltaics onto thin tubular light pipes, the optical energy can be effectively captured within the absorbing layer without associated reflective losses at the front and rear surfaces of the devices as is typical in planar structures. We have used a common absorber system: poly-3-hexyl-thiophene:phenyl-C₆₁-butyric-acid-methyl-ester to demonstrate these tubular optical geometries result in very little overall radiative loss. Surprisingly, this also leads to an overall broadening of the absorption window for the device as indicated by the external quantum efficiency. © 2010 American Institute of Physics. [doi:10.1063/1.3453757]

Recently, several groups have reported advances in the synthesis of small-band-gap conjugated polymers¹⁻⁴ that promise to significantly broaden the spectral overlap of organic photovoltaics absorbers. Poly(5,7-bis(4-decanyl-2-thienyl)-thieno(3,4-b)diathiazole-thiophene-2,5) for example, has a spectral response from 300 to 1450 nm and exceptional internal quantum conversion efficiency.⁵ These low band gap polymers have already demonstrated efficiencies in planar devices exceeding 6.7%.⁶⁻⁸ However, if one determines the total number of photons in the spectrum between 300 and 1450 nm, and then assumes each photon could result in one electron-hole pair, then efficiencies much higher than this should be expected. Indeed, efficiencies greater than 14% should be easily achieved. So why is not this the case? A significant drawback to the use of any polymer absorber is that reflections at the surfaces and interference effects within the thin film prevent light from being absorbed, what is needed is an optical geometry that allows for all of the light within the absorption band to be captured.

This optical geometry can be achieved by “wrapping” the solar cell around a tubular cavity. Similar in design to the fiber-based photovoltaics (PV) which have recently been reported,⁹⁻¹³ tube-based photovoltaics (TBPV) have no loss by reflection at the front surface. Further, due to the special “tube structure,” light will be continuously transmitted down the tube and be completely absorbed. We note that this is quite different from absorbing light along the outer surface of a large cylinder, tube as in the case of Solyndra's devices.¹⁴ While we use thin films of poly-3-hexylthiophene:phenyl-C₆₁-butyric acid methylester (P3HT:PCBM) to demonstrate the function of TBPVs, the light confinement principles can be applied to any absorber. Thus, it represents a general approach to dealing with the thin-film effects in organic PVs.

TBPV devices were fabricated on glass tubes with one end closed in a hemispherical cap [Chemglass, 0.8 mm inner

diameter, 0.25 mm wall, 1.3 mm outer diameter (OD)]. The tubes were cleaned in an ultrasonic bath and were then exposed to ozone for 90 min (rotating the tubes three times after every 30 min). Subsequently, by a dip coating procedure (Opticer H10 Dip Coater), poly(3,4-ethylenedioxythiophene)-poly(styrenesulfonate) (PEDOT:PSS, ClevisTM PH 750, conductive, thickness ~200 nm), P3HT:PCBM (1:0.8 in WT, of 12 mg/ml in chlorobenzene, thickness ~80 nm) were deposited on the tubes. Conductive PEDOT was used in place of the standard indium tin oxide (ITO) due to ease of processing (dip coating) and quality of the final film. Finally, Al electrodes were deposited via thermal evaporation at the pressure of 10⁻⁶ torr. Contacts were silver pasted onto the tube. The length of the tube with active area was about 4 cm. The resulting device structure is shown in Fig. 1.

TBPV devices were tested using an AM1.5g standard Newport No. 96000 Solar Simulator with an illumination intensity of 100 mW/cm². The open end of the tubes was illuminated. Current voltage characteristics were collected using Keithley 236 source-measurement unit. The transmittance spectra of all films were characterized by an UV-Vis Spectrophotometer Varian, Cary 50. The external quantum efficiency (EQE) was measured using a Newport Corner-

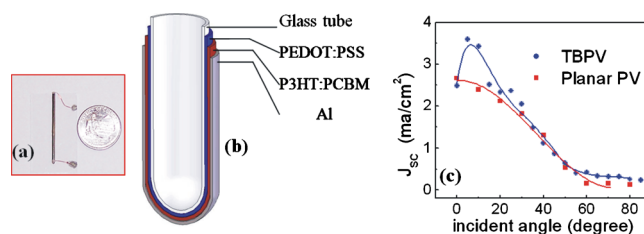


FIG. 1. (Color online) (a) is the schematic of the TBPV architecture and light illumination (longitudinal section) and (b) is a photographic image of the TBPV device. Since the closed end face is silvered by Al, the light will reflect on this curved end face and continue to transmit back up the tube to be absorbed. (c) Comparison of the J_{sc} for TBPV and planar PV as a function of the incident angle.

^{a)}Electronic mail: carrolldl@wfu.edu. Tel. +1-(336) 727-1806.

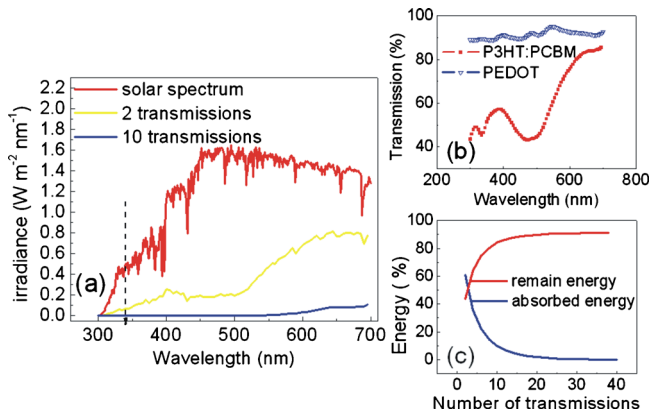


FIG. 2. (Color online) (a) A comparison of the solar spectrum as it transmits through the layers of the two PVs. The curve (two transmissions) corresponds to the solar energy remaining after a single reflection through a planar device. The curve (ten transmissions) represents the remaining solar energy after the light is transmitted down a TBPV once. (b) The transmission spectrum of P3HT:PCBM, and PEDOT used to compute the curves of (a). (c) Shows that the energy absorbed by multiple transmissions through the P3HT:PCBM layer (bottom line) in the TBPV grows quickly as a function of internal reflections in the device. The remaining light energy in tube (top line), shows the corresponding decrease to zero.

stone 260 Monochromator in conjunction with a Newport 300 W Xenon light source. Apertures ensured that side illumination did not occur. Planar PVs were fabricated on glass using the usual spin casting techniques as a control, and tested used the same configuration of polymers with no ITO to ensure an accurate comparison.

Using the transmission spectrum [Fig. 2(b)] of each material with thicknesses of device and an iterative approach [Fig. 2(a) and Eq. (1)], we can estimate how much energy will be absorbed by continuous transmission and absorption in a TBPV comparing with planar PV in Fig. 2(a). As would be expected significantly more light than the planar device should be absorbed. In terms of this method, there is 35% energy that is not absorbed in thin film planar PV in Fig. 2(c) but is utilized by TBPV. If we assume that the TBPV and the planar PV can be made with the same overall voltages and filling factors then the efficiencies of the devices, defined as the open circuit voltage (V_{oc}) times the filling factor (FF) times the short circuit current density (J_{sc}) divided by the input solar power: $(V_{oc} \times FF \times J_{sc})/\text{solar power}$, can be divided such that the ratio of efficiencies between the two devices is simply the ratio of their absorbed energies. This too assumes that the conversion of absorbed photons into current is the same for both cases. In fact this yields an underestimate of the advantages of TBPV since photons emitted by radiative recombination can have a greater chance of being absorbed due to the confined nature of the tube geometry as opposed to the open nature of the planar PV. Neglecting this correction, Eq. (1) is a simple expression for the efficiency of TBPV could be obtained by

$$f_{\text{efficiency of TBPV}} = \frac{\sum_{\text{each wavelength}} [A(2-A)]^{-1} S}{\sum_{\text{each wavelength}} S} f_{\text{efficiency of planar PV}}(A), \quad (1)$$

where, $f_{\text{efficiency of TBPV}}$ is the estimated maximum efficiency for TBPV in terms of the efficiency of planar PV that uses the same materials as the TBPV. The total absorption spec-

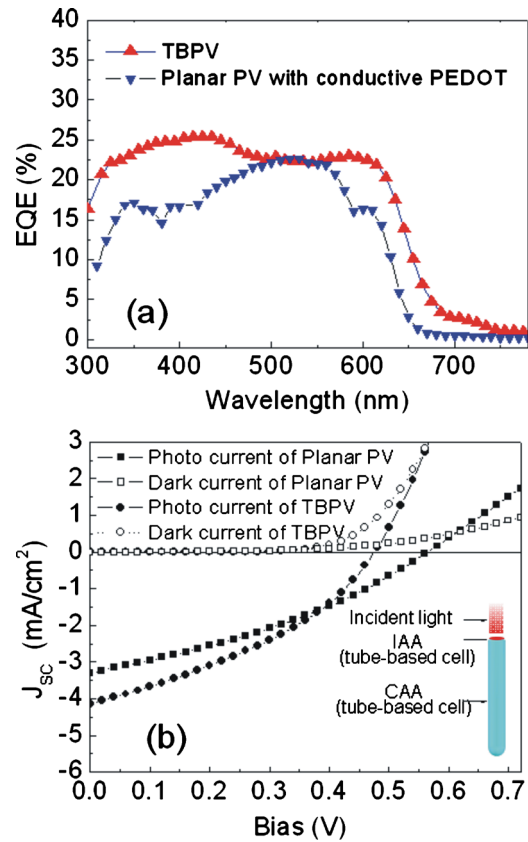


FIG. 3. (Color online) (a) EQE vs wavelength of the two PVs: (down triangle) planar PV with conductive PEDOT/P3HT:PCBM/Al; (upper triangle) TBPV with conductive PEDOT/P3HT:PCBM/Al. The improvement of current generated by this EQE is about 30% relative to planar PV. (its corresponding current density changes from 3.1 mA/cm² to 4.1 mA/cm²). (b) J-V characteristics of TBPV and planar PV (center), and active area explanations (bottom right corner). The current density of short circuit is defined as $J_{sc} = I_{sc}/A_{ea}$, where A_{ea} is the IAA. This is a device current density. The power conversion efficiencies of the solar cells are given as: TBPV $J_{sc} = 3.5$ mA/cm², $V_{oc} = 0.475$ V, FF=0.37, and $\eta_e = 0.60\%$; planar PV $J_{sc} = 2.8$ mA/cm², $V_{oc} = 0.565$ V, FF=0.34, and $\eta_e = 0.52\%$. Current improvement is 25%, and efficiency improvement is 15%.

trum $A = \sum_i a_i$, where a_i is an absorption spectrum (expressed as a vector) of material i . S is the solar spectrum. n is the transmission times. (A complete derivation is provided in the supplemental information available on line. See Ref. 15 for equations derivation.)

Using the Eq. (1), and the efficiency of planar PV with the same layers [$\eta_e = 0.52\%$; in Fig. 3(b)], the efficiency of the equivalent TBPV can be calculated to be $\eta_{e_max} = 0.80\%$. Keep in mind this is a relative efficiency based upon PEDOT/PCBM:P3HT absorbers on glass using no ITO and with relatively low filling factors and no annealing. The improvement in the performance due to changes in the optical architecture is striking.

An important and significant prediction that can be made from this analysis is that the TBPV should absorb far more light at the band edges of the polymer. In the case of P3HT:PCBM systems, this increased absorption will occur between 600 and 700 nm. Typically, these states would be filled with relatively nonmobile charge, and thus not contribute much to the overall power generation. To see if this is the case, we measured the EQE of the TBPV and planar PV devices using the same materials in Fig. 3(a). Across most of the absorption spectrum we see enhanced power generation

for the TBPV as should be expected from its greater ability to capture and retain the solar flux. The improvement of current generated by EQE from 300 to 800 nm is about 30% relative to planar PV. We also see that power generation occurs at longer wavelengths for the tubular devices than for the planar devices. This suggests that the band edge absorption in the TBPV is capable of generating current (and thus power), a quite unexpected result.

With the broadening of the EQE spectrum in the TBPV, as shown in Fig. 3(a), a significant increase in overall device performance is expected. Shown in Fig. 3(b) (the light and dark curves of the TBPV as compared to the planar PV), the current improvement is 25%, and the efficiency improvement is 15%. To understand exactly how these were determined, we must introduce definitions for the two kinds of “active areas” in the TBPV: the “current active area” (CAA) and “illumination active area” (IAA). In Fig. 3(b), the solar light enters the tube from the top open end face (IAA = $\pi OD^2/4 \approx 0.01 \text{ cm}^2$) and to be absorbed on the side face of tube (CAA = $\pi OD \cdot \text{tubelength} + 2 \pi (OD/2)^2 = 1.66 \text{ cm}^2$). In addition, if the tubes are bundled together, it is necessary to take into account the area of gap between each tubes. Thus, $CAA_{\text{all}} = n \times CAA_{\text{single}} + n \times \text{gap}$, and IAA = area of substrate supporting bundles. In sum, CAA is a concept we defined for three-dimensional structure PV, such as tube-based solar cell, fiber-based solar cell, fiber bundles, etc.¹¹ Therefore, the currents in a TBPV can be high relative to the planar PV because the current generated by CAA is divided by IAA. This is done in the same fashion as previously reported for fiber-based PVs.¹² Of course it must be stated that making the tube too long results in all of the light being lost in the first few millimeters of the device, leaving the back of the device to produce no current. Consequently, the V_{oc} is lowered for devices that are too long (decreases 0.1 V). In our work relatively long devices were used for ease of handling and we do see a corresponding drop in voltage.

From the above prediction, we expect an efficiency improvement of roughly 1.5 times due to the enhanced absorption properties of the TBPV device. This corresponds reasonably well to the 1.3 times improvement in current generation. However in this example the fill factor, and the open circuit

voltage of two devices are different (as explained above) which reduces the total increase in performance of the TBPV relative to the planar PV, though a significant increase in performance is seen.

In summary, we have demonstrated an approach to addressing issues of light absorption in organic PVs with tube-based architecture. Unexpectedly, this architecture is able to “broaden” the absorption range of a given polymer by producing power from band edge absorption. The demonstration here utilizes P3HT:PCBM, a common bulk heterojunction system that has been widely studied. However, if this architecture is applied to the high performance low band gap polymers being developed today, these results suggest that the immediate result would be to produce organic solar cells that approach 10%, a number that is competitive in today’s thin film solar cell market.

¹S. H. Park, A. Roy, S. Beaupre, S. Cho, N. Coates, J. S. Moon, D. Moses, M. Leclerc, K. Lee, and A. J. Heeger, *Nat. Photonics* **3**, 297 (2009).

²H. Y. Chen, J. H. Hou, S. Q. Zhang, Y. Y. Liang, G. W. Yang, Y. Yang, L. P. Yu, Y. Wu, and G. Li, *Nat. Photonics* **3**, 649 (2009).

³L. J. Huo, J. H. Hou, H. Y. Chen, S. Q. Zhang, Y. Jiang, T. L. Chen, and Y. Yang, *Macromolecules* **42**, 6564 (2009).

⁴R. C. Coffin, J. Peet, J. Rogers, and G. C. Bazan, *Nat. Chem.* **1**, 657 (2009).

⁵X. Gong, M. Tong, Y. Xia, W. Cai, J. S. Moon, Y. Cao, G. Yu, C.-L. Shieh, B. Nilsson, and A. J. Heeger, *Science* **325**, 1665 (2009).

⁶J. Y. Kim, K. Lee, N. E. Coates, D. Moses, T. Q. Nguyen, M. Dante, and A. J. Heeger, *Science* **317**, 222 (2007).

⁷S. Sista, M.-H. Park, Z. Hong, Y. Wu, J. Hou, W. L. Kwan, G. Li, and Y. Yang, *Adv. Mater.* **22**, 380 (2010).

⁸Y. Y. Liang, Y. Wu, D. Q. Feng, S. T. Tsai, H. J. Son, G. Li, and L. P. Yu, *J. Am. Chem. Soc.* **131**, 56 (2009).

⁹J. W. Liu, M. A. G. Namboothiry, and D. L. Carroll, *Appl. Phys. Lett.* **90**, 133515 (2007).

¹⁰J. W. Liu, M. A. G. Namboothiry, and D. L. Carroll, *Appl. Phys. Lett.* **90**, 063501 (2007).

¹¹Y. Li, W. Nie, J. Liu, A. Partridge, and D. L. Carroll, *IEEE J. Sel. Top. Quantum Electron.* **99**, 1 (2010).

¹²Y. Li, W. Zhou, D. Xue, J. W. Liu, E. D. Peterson, W. Y. Nie, and D. L. Carroll, *Appl. Phys. Lett.* **95**, 203503 (2009).

¹³B. O’Connor, K. P. Pipe, and M. Shtein, *Appl. Phys. Lett.* **92**, 193306 (2008).

¹⁴Proprietary cylindrical modules by Solyndra, <http://www.solyndra.com/Products/More-Electricity>.

¹⁵See supplementary material at <http://dx.doi.org/10.1063/1.3453757> for equations derivation.